Published in final edited form as:
J Neurochem. 2011 November ; 119(3): 594–603. doi:10.1111/j.1471-4159.2011.07456.x.

Diabetic Neuropathy Enhances Voltage–Activated Ca^{2+} Channel Activity and Its Control by M_4 Muscarinic Receptors in Primary Sensory Neurons

Xue-Hong Cao, **Hee Sun Byun**, **Shao-Rui Chen**, and **Hui-Lin Pan**
Department of Anesthesiology and Perioperative Medicine (XHC, HSB, SRC, and HLP), The University of Texas MD Anderson Cancer Center Houston, TX 77030, and, Programs in Neuroscience and Experimental Therapeutics (HLP) The University of Texas Graduate School of Biomedical Sciences Houston, TX 77225

Abstract

Painful neuropathy is one of the most serious complications of diabetes and remains difficult to treat. The muscarinic acetylcholine receptor (mAChR) agonists have a profound analgesic effect on painful diabetic neuropathy. Here we determined changes in T-type and high voltage-activated Ca^{2+} channels (HVACCs) and their regulation by mAChRs in dorsal root ganglion (DRG) neurons in a rat model of diabetic neuropathy. The HVACC currents in large neurons, T-type currents in medium and large neurons, the percentage of small DRG neurons with T-type currents, and the Cav3.2 mRNA level were significantly increased in diabetic rats compared with those in control rats. The mAChR agonist oxotremorine-M significantly inhibited HVACCs in a greater proportion of DRG neurons with and without T-type currents in diabetic than control rats. In contrast, oxotremorine-M had no effect on HVACCs in small and large neurons with T-type currents and in most medium neurons with T-type currents from control rats. The M_2 and M_4 antagonist himbacine abolished the effect of oxotremorine-M on HVACCs in both groups. The selective M_4 antagonist muscarinic toxin-3 caused a greater attenuation of the effect of oxotremorine-M on HVACCs in small and medium DRG neurons in diabetic than control rats. Additionally, the mRNA and protein levels of M_4, but not M_2, in the DRG were significantly greater in diabetic than control rats. Our findings suggest that diabetic neuropathy potentiates the activity of T-type and HVACCs in primary sensory neurons. M_4 mAChRs are upregulated in DRG neurons and probably account for increased muscarinic analgesic effects in diabetic neuropathic pain.

Introduction

Peripheral neuropathy is one of the most serious complications of diabetes. Diabetic neuropathy is frequently painful that typically involves the extremities, occurring as an exaggerated response to either a painful stimulus (hyperalgesia) or a mild and normally nonpainful stimulus (allodynia) (Clark and Lee 1995; Veves et al. 2008). Existing therapies for this devastating complication of diabetes are largely inadequate. The cholinergic system and muscarinic acetylcholine receptors (mAChRs) are critically involved in the control of pain transmission. For example, blocking mAChRs with atropine causes a large increase in pain sensitivity (Zhuo and Gebhart 1991). Furthermore, intrathecal injection of mAChR agonists or acetylcholinesterase inhibitors produces potent analgesia in animal models

Address for correspondence: Hui-Lin Pan, M.D., Ph.D., Department of Anesthesiology and Perioperative Medicine, Unit 110, The University of Texas MD Anderson Cancer Center, 1515 Holcombe Blvd., Houston, TX 77030; Tel: (713) 563-0822; Fax: (713) 794-4590; huilinpan@mdanderson.org.

The authors declare that they have no conflict of interest regarding the work presented here.

(Smith et al. 1989; Naguib and Yaksh 1994; Chen and Pan 2003). Spinally administered neostigmine has been used to effectively treat patients with various pain conditions (Hood et al. 1997; Nakayama et al. 2001). The acetylcholinesterase inhibitor or mAChR agonist has a profound analgesic effect in a rat model of painful diabetic neuropathy (Chen et al. 2001; Chen and Pan 2003). Nevertheless, little is known about how diabetic neuropathy affects the mAChR function in primary sensory neurons.

Five molecularly distinct mAChR subtypes (M_1–M_5) have been identified and divided into two functional classes according to their G-protein coupling preference (Caulfield 1993; Wess 1996). The M_1, M_3 and M_5 subtypes selectively couple to the G_q/G_{11} family of G proteins, whereas the M_2 and M_4 subtypes mainly couple to G_i/G_o family of G proteins (Caulfield 1993; Wess 1996). M_2–M_5 mAChR subtypes play an important role in the control of glutamatergic synaptic transmission and nociception at the spinal level (Gomeza et al. 1999; Chen et al. 2005; Zhang et al. 2007a; Cai et al. 2009; Chen et al. 2010). Both M_2 and M_4 subtypes are expressed in dorsal root ganglion (DRG) neurons (Bernardini et al. 1999; Cai et al. 2009). Although M_2 is the most abundant mAChR subtype in the DRG (Bernardini et al. 1999; Tata et al. 2000; Cai et al. 2009), stimulation of M_4 subtype also reduces nociception (Ellis et al. 1999; Duttaroy et al. 2002; Cai et al. 2009). It remains unclear about the relative changes in M_2 and M_4 subtypes in DRG neurons and their contribution to muscarinic analgesia in painful diabetic neuropathy.

Voltage-activated Ca^{2+} channels (VACCs) are critically involved in the regulation of neurotransmitter release. We have shown that μ-opioid agonist inhibits high voltage-activated Ca^{2+} channels (HVACCs) only in small DRG neurons devoid of T-type VACCs (Wu et al. 2009). However, it is unclear whether the inhibitory effect of the mAChR agonist on HVACCs is present in DRG neurons with T-type VACCs. Therefore, in the present study, we determined the relationship between inhibition of HVACCs by mAChR activation and the presence of T-type VACCs in DRG neurons in a rat model of diabetic neuropathy. Furthermore, using the HVACCs as a functional readout, we tested the hypothesis that the activity of M_2 and M_4 subtypes is upregulated in DRG neurons in diabetic neuropathy.

Materials and Methods

Animal model of diabetic neuropathic pain

All experiments were approved by the Animal Care and Use Committee of the University of Texas MD Anderson Cancer Center and conformed to the guidelines of the National Institutes of Health's Guide for the Care and Use of Laboratory Animals. Male Sprague-Dawley rats (9 weeks old, Harlan Sprague-Dawley, Indianapolis, IN) were used. Experimental diabetes was induced by administration of a single dose streptozotocin (STZ, 60 mg/kg, i.p) (Chen and Pan 2002; Cao et al. 2010). This low dose of STZ was used to minimize the effect of STZ on the overall health of the animal (Chen and Pan 2002, 2003). This animal model mimics the symptoms of neuropathy in diabetic patients and shows increased pain sensitivity and poor responses to μ opioid agonists administered systemically or intrathecally (Courteix et al. 1993; Malcangio and Tomlinson 1998; Chemin et al. 2002). Early insulin treatment can prevent or impede the development of painful diabetic neuropathy induced by STZ in rats (Sasaki et al. 1998; Hoybergs and Meert 2007). Age-matched saline-injected rats were used as the controls. Three weeks after STZ injection, diabetes was confirmed by testing the glucose concentration in the tail vein blood using ACCU-CHEK test strips (Roche Diagnostics, Indianapolis, IN). Neuropathic pain in diabetic rats was confirmed by examining nociceptive thresholds using the paw pressure test (Analgesy-Meter, Ugo Basile Biological Research, Comerio, Italy) (Chen and Pan 2002, 2006). All the diabetic rats remained relatively healthy except that their growth rate was reduced (body weight gain: 5 g/week in the diabetic group versus 20 g/week in the

nondiabetic group). The final electrophysiological experiments were performed on rats 3 weeks after STZ or vehicle treatment.

Dissociation of DRG neurons

Rats were anesthetized with 2–3% isoflurane and then rapidly decapitated. The lumbar DRGs were quickly dissected out and transferred immediately into cold Dulbecco's medium (DMEM; Gibco, Carlsbad, CA). DRG neurons were dissociated enzymatically as we described previously (Wu et al. 2009; Cao et al. 2010). The cell suspension was platted onto a 35-mm culture dish containing poly-L-lysine (50 μg/ml) pre-coated coverslips and incubated in 5% CO_2 at 37°C for 1 hr. DRG neurons were kept in the incubator for at least another hour before they were used for electrophysiological recordings.

Electrophysiological recordings of calcium currents

The recording electrodes (resistance, 1–4 MΩ) were pulled and fire-polished. The neurons were visualized using differential interference contrast optics on an inverted microscope (Olympus, Tokyo, Japan). Images of the cells were taken with a CCD camera and displayed on a video monitor. The neurons were recorded in the whole-cell configuration using an EPC-10 amplifier (HEKA Instruments, Lambrecht, Germany). Signals were filtered at 2 kHz and digitized at 10 kHz. Whole-cell series resistance was electronically compensated, and the leak currents were subtracted using the online P/4 protocol. All experiments were performed within 7 hours at room temperature (about 25°C) after DRG dissociation.

VACC currents were measured using barium as the charge carrier (I_{Ba}). The extracellular solution consisted of (in mM) 140 tetraethylammonium chloride, 2 $MgCl_2$, 3 $BaCl_2$, 10 glucose, and 10 HEPES (pH 7.4 adjusted with tetraethylammonium hydroxide; osmolarity, 320 mOsm). The pipette internal solution contained (in mM) 120 CsCl, 1 $MgCl_2$, 10 HEPES, 10 EGTA, 2 Mg-ATP, and 0.1 Na-GTP (pH 7.2 adjusted with CsOH; osmolarity 300 mOsm). GTP and ATP were included in the pipette solution to minimize the "run-down" of VACC currents associated with the whole-cell recording (Wu et al. 2009). The stock drug solutions were diluted in the appropriate external solution immediately before use and held in a series of independent syringes connected to corresponding fused silica columns. All drugs and chemicals were purchased from Sigma-Aldrich except muscarinic toxin-3 (MT-3), which was obtained from Peptide Institute, Inc (Osaka, Japan).

Real-time PCR analysis of M_2, M_4, Cav3.2, and Cav3.3 mRNA levels

Total RNA was extracted from rat lumbar DRGs at the L4–L6 level using the Purelink total RNA purification system (Invitrogen, Carlsbad, CA) with on-column DNase I digestion according to the manufacturer's instructions. cDNA was prepared by using the Superscript III first-strand synthesis kit (Invitrogen, Carlsbad, CA). Quantitative PCR was performed using the iQ5 real-time PCR detection system with the SYBR green PCR kit (Bio-Rad, Hercules, CA). All samples were analyzed in duplicate using an annealing temperature of 60°C, and each experiment was repeated at least once. The primer pairs used are listed in Table 1. The relative mRNA amount of M_2, M_4, Cav3.2, and Cav3.3 in each sample was first normalized to the level of the housekeeping gene GAPDH and was then normalized to its expression level in control rats (the mean values of M_2, M_4, Cav3.2, and Cav3.3 in control rats were considered to be 1). The PCR product specificity was verified by melting-curve analysis and agarose gel electrophoresis (Cai et al. 2009).

Western blot analysis of M_2 and M_4 protein levels in the DRG

To quantify the protein level of M_2 and M_4 subtypes in the DRGs, rats were anesthetized by 2–3% isoflurane and decapitated. Both sides of DRGs at the L4–L6 level were quickly

collected and homogenized in ice-cold buffer containing 20 mM Tris (pH 7.6), 0.5% NP-40, 250 mM NaCl, 3 mM EDTA, 3 mM EGTA, 2 mM DTT, 10% sucrose, and the protease inhibitor cocktail (Sigma). The homogenate was centrifuged at 12,000×g for 20 min at 4°C. The supernatant was collected and the protein concentration was determined using the Lowry protein assay. For Western blotting, 50 μg proteins was separated by 10% SDS–polyacrylamide gel electrophoresis and transferred to a PVDF membrane (Millipore). The membrane was blocked for 30 min in 5% skim milk in phosphate-buffered saline containing 0.05% Tween-20 and then incubated with rabbit anti-M_2 and rabbit anti-M_4 primary antibodies (from Dr. Jürgen Wess, NIDDK/NIH) for overnight at 4 C. The specific protein band of M_4 was confirmed by using CCD-1064Sk whole-cell lysate as a positive control, because M_4 protein is present in this cell lysate (Santa Cruz Biotechnology, sc-2263). The membrane was then rinsed and incubated with horseradish peroxidase-conjugated anti-rabbit secondary antibody (Jackson ImmunoResearch) at 1:10,000 dilutions for 1 hr at room temperature. The membrane was developed with an enhanced chemiluminescence kit according to the manufacturer's instructions. For the protein loading control, membranes were also incubated with a mouse anti-β actin antibody (Sigma). The intensity of protein bands was captured digitally and analyzed quantitatively with AIS software (Imaging Research Inc., London, UK).

Data analysis

Data were presented as means ± SEM. Unpaired Student's *t*-test was used to examine the difference in the current density of T-type and HVACC I_{Ba} between the control and diabetic group. The activation (τ_m) and inactivation (τ_h) constants of the HVACC currents were calculated by fitting the current (I) with the following Hodgkin-Huxley relation: $I_{max}(t) = A(1\text{-}e^{(-t/\tau_m)})^P (h_{inf} - (h_{inf} - 1)\, e^{(-t/\tau_h)})$, where A indicates the voltage-depending part of the current, p is the exponent of m, hinf is the equilibrium value reached by h according to the potential, and t is the time (in ms). Cells were considered as having T-type currents if the amplitude of I_{Ba} at −45 mV was more than 20 pA. Also, cells were considered as responsive to Oxo-M if the peak amplitude of I_{Ba} was reduced more than 15% during Oxo-M application. Chi-square test was used to determine the difference in the percentage of the cells inhibited by Oxo-M between the control and diabetic groups. One-way ANOVA test was used to determine the contribution of M_2 or M_4 subtype to the inhibition of HVACC I_{Ba} by Oxo-M, and two-way ANOVA was used to examine the difference in dose-dependent inhibition of HVACC I_{Ba} by Oxo-M between the control and diabetic groups. $P < 0.05$ was considered to be statistically significant.

Results

Three weeks after diabetic induction, the diabetic rats showed a significant reduction in the paw withdrawal threshold in response to the pressure stimulus applied to the hindpaw, compared with that in control rats (control rats: 122.67 ± 2.67 g; diabetic rats: 77.33 ± 2.06 g, $P < 0.05$).

The DRG neurons obtained from control and diabetic rats were divided into three groups according to their cell diameters measured with a calibrated eyepiece reticule: small (< 30 μm), medium (30–40 μm), and large (> 40 μm) (Cao et al. 2010). To determine the whole-cell I_{Ba} currents in these three groups of DRG neurons, we normalized the peak inward current to the cell capacitance.

Changes in T-type and HVACC currents in different sizes of DRG neurons in diabetic rats

To measure the T-type and HVACC currents in DRG neurons, neurons were voltage clamped at −90 mV and depolarized to −45 mV (T-type I_{Ba}) for 200 ms followed by a pulse

from −90 mV to 0 mV (HVACC I_{Ba}) for 200 ms at 1-s intervals (Wu et al. 2009). The percentage of small, DRG neurons with T-type I_{Ba} was significantly increased in diabetic rats (26/86, 30.2%) compared with that in control rats (21/149, 14.1%, Fig. 1, A–C). However, the percentage of medium (control: 51/101, 50.50%; diabetic: 34/80, 42.50%) and large (control: 4/54, 7.41%; diabetic: 4/38, 10.53%) DRG neurons with T-type I_{Ba} did not differ significantly between the two groups. In addition, the T-type I_{Ba} current density was significantly increased in medium and large, but not small, DRG neurons in the diabetic group compared with the control group (Fig. 1D).

The HVACC current density was significantly increased in large DRG neurons in diabetic rats compared with that in control rats (Fig. 1E). However, there were no significant differences in the HVACC current density in small and medium DRG neurons between control and diabetic rats.

Changes in the mRNA level of Cav3.2 and Cav3.3 subunits in the DRG from diabetic rats

We next determined changes in the mRNA level of Cav3.2 and Cav3.3 subunits in the DRG of control and diabetic rats, because Cav3.1 mRNA is not present in the DRG (Talley et al. 1999). Quantitative PCR analysis revealed that the Cav3.2 mRNA level was increased about 30% in the DRG from diabetic rats compared with that from control rats (Fig. 1F). However, the mRNA level of Cav3.3 subunit in the DRG did not differ significantly between the control and diabetic group (Fig. 1F).

Effects of mAChR activation on I_{Ba} currents in different sizes of DRG neurons in diabetic rats

To determine the effect of mAChR activation on HVACCs in DRG neurons, we used oxotremorine-M (Oxo-M), a nonselective agonist for all mAChR subtypes. Oxo-M at 0.1, 0.3, 1, and 3 μM was bath applied to the neuron, and each concentration was applied for 2 min. In control rats, Oxo-M significantly inhibited HVACC I_{Ba} in 19/67 (28.36%) small, 12/51 (23.53%) medium, and 4/45 (8.89%) large DRG neurons in a dose-dependent manner. Oxo-M inhibited HVACC I_{Ba} in a significantly greater proportion of DRG neurons in diabetic (small, 22/44, 50%; medium, 28/46, 60.87%; large, 12/29, 41.38%) than in control rats. However, the degree of inhibition of HVACC I_{Ba} by Oxo-M in DRG neurons responsive to Oxo-M did not differ significantly between control and diabetic rats (Figs. 2–4, A–C). In all of the DRG neurons in which the effect of 1 μM Oxo-M on I_{Ba} was examined, Oxo-M inhibited HVACC I_{Ba} in a significantly greater proportion of different sizes of neurons in diabetic group (small: 44/85, 51.16%; medium: 50/80, 62.50%; large: 17/38, 44.74%), compared with that in control group (small: 40/149, 26.85%; medium: 29/101, 28.71%; Large: 7/54, 12.96%; Figs. 2–4, D,E). The inactivation time constant of HVACC currents was faster in diabetic than in control rats (Fig. 2F). Also, Oxo-M significantly increased the activation time constant of HVACCs in both control and diabetic rats (Fig. 2G).

Oxo-M (1 μM) had no significant effect on the T-type I_{Ba} in all of the DRG neurons tested from the control and diabetic rats (Fig. 5, A and B). Also, in neurons with T-type I_{Ba} in control rats, Oxo-M failed to inhibit HVACC I_{Ba} in any small or large DRG neurons. However, Oxo-M inhibited HVACC I_{Ba} in 4/51 (7.84%) medium DRG neurons obtained from control rats. In contrast, 1 μM Oxo-M inhibited HVACC I_{Ba} in a significantly greater portion of DRG neurons with T-type I_{Ba} in diabetic rats (small: 7/26, 26.92%; medium: 10/34, 29.41%; large: 1/4, 25%; Fig. 5C).

Contribution of M_2 and M_4 subtypes to inhibition of HVACCs by Oxo-M in DRG neurons from diabetic rats

To assess the contribution of M_2 and M_4 subtypes to Oxo-M-induced inhibition of HVACCs, we took advantage of MT-3, a highly specific blocker for M_4 subtype (Ellis et al. 1999; Zhang et al. 2005), and himbacine, a selective antagonist for both M_2 and M_4 subtypes (Miller et al. 1992; Zhang et al. 2005). The appropriate concentrations of MT-3 (50 nM) and himbacine (2 μM) have been validated using M_2 single-knockout and M_2/M_4 double-knockout mice (Zhang et al. 2005; Zhang et al. 2007b; Chen et al. 2010). First, we tested whether 1 μM Oxo-M inhibited HVACC I_{Ba}. Then, we examined whether MT-3 (50 nM) attenuated the inhibitory effect of Oxo-M to define the contribution of M_4 subtype. Inhibition of HVACC I_{Ba} by mAChRs is mediated by M_2 and M_4 subtypes, which was confirmed by the complete block of Oxo-M's effect by 2 μM himbacine at the end of the experiments (Fig. 6). Thus, the contribution of M_2 subtype to the inhibitory effect of Oxo-M was estimated by subtraction of MT-3's effect from the total inhibitory effect of Oxo-M on HVACC I_{Ba}. We normalized M_2- and M_4-mediated inhibition of HVACCs using the initial inhibition of HVACC I_{Ba} produced by 1 μM Oxo-M in individual DRG neurons.

In small DRG neurons, M_4-mediated inhibition of HVACC I_{Ba} was significantly increased in the diabetic group (61.19 ± 6.13%, n = 16) compared with that in the control group (36.86 ± 5.07%, n = 14; $P < 0.05$, Fig. 6, A–C). However, the M_2-mediated inhibition of HVACC I_{Ba} (control: 60.37 ± 4.55%; diabetic: 49.41 ± 8.82%) in small DRG neurons did not differ significantly between control and diabetic rats (Fig. 6, A–C).

Similarly, M_4-mediated inhibition of HVACC I_{Ba} in medium DRG neurons was also significantly greater in diabetic than control rats (control: 45.04 ± 10.03%, n = 12; diabetic: 74.49 ± 7.06%, n = 8, $P < 0.05$, Fig. 6D). However, M_2-mediated inhibition of HVACC I_{Ba} in these DRG neurons did not differ significantly between control and diabetic rats (control: 45.96 ± 10.75%; diabetic: 28.51 ± 10.06%; Fig. 6D).

In both control and diabetic rats,1 μM Oxo-M inhibited HVACC I_{Ba} in only a few large DRG neurons. There were no significant differences in M_2- and M_4-mediated inhibition of HVACC I_{Ba} in large DRG neurons between diabetic (M_2: 62.62 ± 9.03%; M_4: 30.26 ± 4.76%; n = 6) and control rats (M_2: 65.24 ± 5.71%, M_4: 28.36 ± 2.09%; n = 5, Fig. 6E).

Changes in the mRNA and protein levels of M_2 and M_4 subtypes in the DRG in diabetic rats

The mRNA level of M_4 subtype in the DRG, measured using quantitative PCR, was significantly increased in diabetic rats compared with that in control rats (Fig. 7). However, the mRNA level of M_2 subtype in the DRG did not differ significantly between the control and diabetic groups.

Also, the protein amount of M_4 subtype in the DRG, quantified using immunoblotting, was significantly increased in diabetic rats compared with that in control rats (Fig. 7). However, the protein level of M_2 subtype in the DRG did not differ significantly between the control and diabetic groups (Fig. 7).

Discussion

In this study, we determined changes in VACCs in different sizes of DRG neurons and the contribution of M_2 and M_4 subtypes to inhibition of VACCs by mAChR activation. We found that T-type VACC current density in medium and large DRG neurons and the proportion of small DRG neurons with T-type I_{Ba} were significantly increased in diabetic rats compared with those in control rats. Also, the HVACC current density in large DRG neurons was significantly increased in diabetic rats compared with that in control rats. We

found that the mAChR agonist Oxo-M inhibited HVACCs in a greater proportion of DRG neurons in diabetic than control rats. Furthermore, M_4 subtype-mediated inhibition of HVACCs by Oxo-M in small and medium DRG neurons was significantly increased in diabetic rats compared with that in control rats. In addition, the mRNA and protein levels of M_4, but not M_2, in the DRG were significantly greater in diabetic than in control rats. Our findings suggest that diabetic neuropathy enhances the activity of VACCs in a population of primary sensory neurons, which may contribute to increased nociceptive input and pain hypersensitivity. Upregulation of M_4 subtype in DRG neurons probably accounts for increased muscarinic analgesic effect in painful diabetic neuropathy.

T-type VACCs can be activated by weak depolarizations and low-threshold spikes, which in turn trigger the burst firing and have a key function in neuronal membrane excitability (Carbone and Lux 1984; Perez-Reyes 2003). T-type VACCs are normally present in DRG neurons associated with D-hair mechanoreceptors (Shin et al. 2003). However, when T-type VACCs are expressed in nociceptive DRG neurons in diabetic neuropathy, they can increase the excitability of these neurons (Jagodic et al. 2007). Gene silencing of the Cav3.2 subtype, which is the predominant T-type subtype in rat DRG neurons (Talley et al. 1999), reduces neuropathic pain caused by diabetic neuropathy and sciatic nerve ligation (Bourinet et al. 2005; Messinger et al. 2009). Consistent with the findings from the previous study (Scroggs and Fox 1992), we found that T-type VACCs were predominantly present in small and medium DRG neurons in control rats. We also found that T-type VACCs were present in more small DRG neurons in the diabetic than control rats. Although the percentage of medium and large DRG neurons with T-type VACCs did not differ between control and diabetic rats, the current density of T-type VACCs was significantly increased in diabetic rats compared with that in control rats. Furthermore, we observed that the mRNA level of Cav3.2, but not Cav3.3, subtype in the DRG was significantly increased in diabetic rats compared with that in control rats. Thus, increased expression and activity of Cav3.2 in DRG neurons could contribute to increased excitability of primary afferent neurons and the development of chronic pain in diabetic neuropathy.

It has been shown that the activity of HVACCs is increased in capsaicin-sensitive DRG neurons in diabetic Bio Bred/Worchester rats compared with that in non-diabetic controls (Hall et al. 1995). In the present study, we found that the HVACC current density was significantly increased in large, but not small and medium, DRG neurons in STZ-induced diabetic rats compared with that in control rats. Also, diabetic neuropathy increased the inactivation time constant of HVACC currents in DRG neurons, which may result from increased expression of different subtypes of HVACCs or changes in trafficking of the auxiliary subunits of HVACCs. Large DRG neurons, which are commonly associated with myelinated afferent fibers, typically transduce vibratory and tactile sensation (Lawson 2002). Recent studies suggest that increased excitability of myelinated afferent fibers and large sensory neurons contributes to tactile allodynia induced by diabetic neuropathy (Khan et al. 2002; Hong and Wiley 2005). Therefore, increased HVACC activity in large DRG neurons could also play a role in abnormal hyperexcitability of myelinated primary afferent nerves and increased neurotransmitter release in the spinal dorsal horn in painful diabetic neuropathy (Chen and Pan 2002; Khan et al. 2002; Wang et al. 2007).

An important new finding of our study is that mAChR activation inhibited HVACCs in a greater proportion of DRG neurons with T-type VACCs in diabetic than control rats. Spinally administrated muscarine produces a profound antinociceptive effect in diabetic rats (Chen and Pan 2003). Also, diabetic neuropathy leads to upregulation of mAChRs in the dorsal spinal cord in rats (Chen and Pan 2003). We found in this study that Oxo-M inhibited HVACC I_{Ba} in a significantly greater proportion of all sizes of DRG neurons with and without T-type VACCs in diabetic than in control rats. Our data clearly suggest that diabetic

neuropathy increases the activity of inhibitory mAChRs present in various types of DRG neurons. Oxo-M caused a kinetic slowing of HVACC activation in DRG neurons, consistent with the inhibition of HVACCs by activation of G_i/G_o-coupled receptors. Interestingly, we found that the mAChR agonist Oxo-M had no effect on T-type currents or HVACC currents with T-type VACCs in any of small and large DRG neurons obtained from control rats. We have shown that μ-opioid receptor agonists inhibits HVACCs only in DRG neurons without T-type VACCs (Wu et al. 2009). The mechanisms underlying the lack of inhibition of HVACCs by mAChR agonists in neurons with T-type VACCs are not clear. It is possible that DRG neurons with T-type VACCs normally do not express M_2 and M_4 subtypes. Also, it has been shown that T-type VACCs are normally associated with D-hair mechanoreceptors (Shin et al. 2003). On the other hand, M_2 and M_4 subtypes may be primarily expressed in nociceptive DRG neurons (Ellis et al. 1999; Duttaroy et al. 2002; Hayashida et al. 2006; Cai et al. 2009). The splice variant of Cav2.2 (N-type) has been reported in DRG neurons (Bell et al. 2004), and the effects of mAChR agonists may depend on the variation of N-type HVACCs. However, stimulation of M_2 and M_4 mAChRs also inhibits L- and P/Q-type HVACCs (Mathie et al. 1992; Jeong and Wurster 1997). Because all the four subtypes of HVACCs are present in DRG neurons, the presence of various splice variants of N-type HVACCs cannot explain the complete lack of effects of mAChR activation on HVACC currents in DRG neurons with T-type currents.

M_2 and M_4 activation inhibits HVACCs, which possibly contribute to the antinociceptive effect of mAChR agonists through attenuation of the excitatory neurotransmitter release from primary afferent terminals (Zhang et al. 2007a). It has been shown that the inhibitory effect of mAChR agonists on VACCs is mediated by pertussis toxin-sensitive $G_{i/o}$ proteins in neonatal DRG neurons (Wanke et al. 1994). HVACCs are inhibited by $G_{i/o}$ protein activation through the release of $G_{\beta/\gamma}$ subunits (Herlitze et al. 1996; Ikeda 1996; Pan et al. 2008). The effect of diabetic neuropathy on the function of M_2 and M_4 subtypes in DRG neurons has not been studied previously. While M_2 subtype is distributed in different sizes of DRG neurons (Hayashida et al. 2006), M_4 subtype seems preferentially present in small and medium DRG neurons (Tata et al. 2000). To determine the contribution of M_2 and M_4 subtypes to increased inhibition of HVACCs by mAChR stimulation in diabetic rats, we used MT-3 and himbacine to assess the role of M_4 and M_2 subtypes. MT-3 is a highly specific blocker for M_4 subtype (Miller et al. 1992; Ellis et al. 1999; Zhang et al. 2005), and himbacine is a potent mAChR antagonist that displays selectivity for M_2 and M_4 subtypes (Miller et al. 1992). We found that M_4-mediated inhibition of HVACCs by Oxo-M was significantly increased in small and medium DRG neurons in diabetic rats. Furthermore, we found that the mRNA and protein levels of M_4, but not M_2, subtype in the DRGs were significantly increased in diabetic rats compared with those in control rats. Interestingly, it has been shown that nerve transection injury primarily upregulates M_2 subtype in small and medium DRG neurons (Hayashida et al. 2006). Our biochemical and electrophysiological data consistently suggest that diabetic neuropathy primarily potentiates the expression and activity of M_4 subtype in DRG neurons.

In summary, our study demonstrates that diabetic neuropathy enhances the activity of T-type VACCs and HVACCs in subpopulations of DRG neurons. Our results also provide new functional evidence for the critical role of M_4 subtype in the muscarinic control of HVACCs in DRG neurons in diabetic neuropathy. Thus, the inhibitory mAChRs, especially the M_4 subtype, represents a potential therapeutic target for treatment of painful diabetic neuropathy.

Acknowledgments

This study was supported by the National Institutes of Health grants GM064830 and NS045602 and the Helen T. Hawkins Endowment to H.L.P. We thank Dr. Jürgen Wess at NIDDK/NIH for providing M_2 and M_4 antibodies used for this work.

References

Bell TJ, Thaler C, Castiglioni AJ, Helton TD, Lipscombe D. Cell-specific alternative splicing increases calcium channel current density in the pain pathway. Neuron. 2004; 41:127–138. [PubMed: 14715140]

Bernardini N, Levey AI, Augusti-Tocco G. Rat dorsal root ganglia express m1-m4 muscarinic receptor proteins. J Peripher Nerv Syst. 1999; 4:222–232. [PubMed: 10642090]

Bourinet E, Alloui A, Monteil A, Barrere C, Couette B, Poirot O, Pages A, McRory J, Snutch TP, Eschalier A, Nargeot J. Silencing of the Cav3.2 T-type calcium channel gene in sensory neurons demonstrates its major role in nociception. Embo J. 2005; 24:315–324. [PubMed: 15616581]

Cai YQ, Chen SR, Han HD, Sood AK, Lopez-Berestein G, Pan HL. Role of M2, M3, and M4 muscarinic receptor subtypes in the spinal cholinergic control of nociception revealed using siRNA in rats. J Neurochem. 2009; 111:1000–1010. [PubMed: 19780895]

Cao XH, Byun HS, Chen SR, Cai YQ, Pan HL. Reduction in voltage-gated K+ channel activity in primary sensory neurons in painful diabetic neuropathy: role of brain-derived neurotrophic factor. J Neurochem. 2010; 114:1460–1475. [PubMed: 20557422]

Carbone E, Lux HD. A low voltage-activated, fully inactivating Ca channel in vertebrate sensory neurones. Nature. 1984; 310:501–502. [PubMed: 6087159]

Caulfield MP. Muscarinic receptors--characterization, coupling and function. Pharmacol Ther. 1993; 58:319–379. [PubMed: 7504306]

Chemin J, Monteil A, Perez-Reyes E, Bourinet E, Nargeot J, Lory P. Specific contribution of human T-type calcium channel isotypes (alpha(1G), alpha(1H) and alpha(1I)) to neuronal excitability. J Physiol. 2002; 540:3–14. [PubMed: 11927664]

Chen SR, Pan HL. Hypersensitivity of spinothalamic tract neurons associated with diabetic neuropathic pain in rats. J Neurophysiol. 2002; 87:2726–2733. [PubMed: 12037174]

Chen SR, Pan HL. Up-regulation of spinal muscarinic receptors and increased antinociceptive effect of intrathecal muscarine in diabetic rats. J Pharmacol Exp Ther. 2003; 307:676–681. [PubMed: 12966147]

Chen SR, Pan HL. Blocking mu opioid receptors in the spinal cord prevents the analgesic action by subsequent systemic opioids. Brain Res. 2006; 1081:119–125. [PubMed: 16499888]

Chen SR, Khan GM, Pan HL. Antiallodynic effect of intrathecal neostigmine is mediated by spinal nitric oxide in a rat model of diabetic neuropathic pain. Anesthesiology. 2001; 95:1007–1012. [PubMed: 11605898]

Chen SR, Wess J, Pan HL. Functional activity of the M2 and M4 receptor subtypes in the spinal cord studied with muscarinic acetylcholine receptor knockout mice. J Pharmacol Exp Ther. 2005; 313:765–770. [PubMed: 15665136]

Chen SR, Chen H, Yuan WX, Wess J, Pan HL. Dynamic control of glutamatergic synaptic input in the spinal cord by muscarinic receptor subtypes defined using knockout mice. J Biol Chem. 2010; 285:40427–40437. [PubMed: 20940295]

Clark CM Jr, Lee DA. Prevention and treatment of the complications of diabetes mellitus. N Engl J Med. 1995; 332:1210–1217. [PubMed: 7700316]

Courteix C, Eschalier A, Lavarenne J. Streptozocin-induced diabetic rats: behavioural evidence for a model of chronic pain. Pain. 1993; 53:81–88. [PubMed: 8316394]

Duttaroy A, Gomeza J, Gan JW, Siddiqui N, Basile AS, Harman WD, Smith PL, Felder CC, Levey AI, Wess J. Evaluation of muscarinic agonist-induced analgesia in muscarinic acetylcholine receptor knockout mice. Mol Pharmacol. 2002; 62:1084–1093. [PubMed: 12391271]

Ellis JL, Harman D, Gonzalez J, Spera ML, Liu R, Shen TY, Wypij DM, Zuo F. Development of muscarinic analgesics derived from epibatidine: role of the M4 receptor subtype. J Pharmacol Exp Ther. 1999; 288:1143–1150. [PubMed: 10027852]

Gomeza J, Shannon H, Kostenis E, Felder C, Zhang L, Brodkin J, Grinberg A, Sheng H, Wess J. Pronounced pharmacologic deficits in M2 muscarinic acetylcholine receptor knockout mice. Proc Natl Acad Sci U S A. 1999; 96:1692–1697. [PubMed: 9990086]

Hall KE, Sima AA, Wiley JW. Voltage-dependent calcium currents are enhanced in dorsal root ganglion neurones from the Bio Bred/Worchester diabetic rat. J Physiol. 1995; 486:313–322. [PubMed: 7473199]

Hayashida KI, Bynum T, Vincler M, Eisenach JC. Inhibitory M2 muscarinic receptors are upregulated in both axotomized and intact small diameter dorsal root ganglion cells after peripheral nerve injury. Neuroscience. 2006; 140:259–268. [PubMed: 16580144]

Herlitze S, Garcia DE, Mackie K, Hille B, Scheuer T, Catterall WA. Modulation of Ca2+ channels by G-protein beta gamma subunits. Nature. 1996; 380:258–262. [PubMed: 8637576]

Hong S, Wiley JW. Early painful diabetic neuropathy is associated with differential changes in the expression and function of vanilloid receptor 1. J Biol Chem. 2005; 280:618–627. [PubMed: 15513920]

Hood DD, Mallak KA, James RL, Tuttle R, Eisenach JC. Enhancement of analgesia from systemic opioid in humans by spinal cholinesterase inhibition. J Pharmacol Exp Ther. 1997; 282:86–92. [PubMed: 9223543]

Hoybergs YM, Meert TF. The effect of low-dose insulin on mechanical sensitivity and allodynia in type I diabetes neuropathy. Neurosci Lett. 2007; 417:149–154. [PubMed: 17412508]

Ikeda SR. Voltage-dependent modulation of N-type calcium channels by G-protein beta gamma subunits. Nature. 1996; 380:255–258. [PubMed: 8637575]

Jagodic MM, Pathirathna S, Nelson MT, Mancuso S, Joksovic PM, Rosenberg ER, Bayliss DA, Jevtovic-Todorovic V, Todorovic SM. Cell-specific alterations of T-type calcium current in painful diabetic neuropathy enhance excitability of sensory neurons. J Neurosci. 2007; 27:3305–3316. [PubMed: 17376991]

Jeong SW, Wurster RD. Muscarinic receptor activation modulates Ca2+ channels in rat intracardiac neurons via a PTX- and voltage-sensitive pathway. J Neurophysiol. 1997; 78:1476–1490. [PubMed: 9310437]

Khan GM, Chen SR, Pan HL. Role of primary afferent nerves in allodynia caused by diabetic neuropathy in rats. Neuroscience. 2002; 114:291–299. [PubMed: 12204199]

Lawson SN. Phenotype and function of somatic primary afferent nociceptive neurones with C-, Adelta- or Aalpha/beta-fibres. Exp Physiol. 2002; 87:239–244. [PubMed: 11856969]

Malcangio M, Tomlinson DR. A pharmacologic analysis of mechanical hyperalgesia in streptozotocin/diabetic rats. Pain. 1998; 76:151–157. [PubMed: 9696468]

Mathie A, Bernheim L, Hille B. Inhibition of N- and L-type calcium channels by muscarinic receptor activation in rat sympathetic neurons. Neuron. 1992; 8:907–914. [PubMed: 1316767]

Messinger RB, Naik AK, Jagodic MM, Nelson MT, Lee WY, Choe WJ, Orestes P, Latham JR, Todorovic SM, Jevtovic-Todorovic V. In vivo silencing of the Ca(V)3.2 T-type calcium channels in sensory neurons alleviates hyperalgesia in rats with streptozocin-induced diabetic neuropathy. Pain. 2009; 145:184–195. [PubMed: 19577366]

Miller JH, Aagaard PJ, Gibson VA, McKinney M. Binding and functional selectivity of himbacine for cloned and neuronal muscarinic receptors. J Pharmacol Exp Ther. 1992; 263:663–667. [PubMed: 1331410]

Naguib M, Yaksh TL. Antinociceptive effects of spinal cholinesterase inhibition and isobolographic analysis of the interaction with mu and alpha 2 receptor systems. Anesthesiology. 1994; 80:1338–1348. [PubMed: 8010479]

Nakayama M, Ichinose H, Nakabayashi K, Satoh O, Yamamoto S, Namiki A. Analgesic effect of epidural neostigmine after abdominal hysterectomy. J Clin Anesth. 2001; 13:86–89. [PubMed: 11331165]

Pan HL, Wu ZZ, Zhou HY, Chen SR, Zhang HM, Li DP. Modulation of pain transmission by G-protein-coupled receptors. Pharmacol Ther. 2008; 117:141–161. [PubMed: 17959251]

Perez-Reyes E. Molecular physiology of low-voltage-activated t-type calcium channels. Physiol Rev. 2003; 83:117–161. [PubMed: 12506128]

Sasaki T, Yasuda H, Maeda K, Kikkawa R. Hyperalgesia and decreased neuronal nitric oxide synthase in diabetic rats. Neuroreport. 1998; 9:243–247. [PubMed: 9507963]

Scroggs RS, Fox AP. Calcium current variation between acutely isolated adult rat dorsal root ganglion neurons of different size. J Physiol. 1992; 445:639–658. [PubMed: 1323671]

Shin JB, Martinez-Salgado C, Heppenstall PA, Lewin GR. A T-type calcium channel required for normal function of a mammalian mechanoreceptor. Nat Neurosci. 2003; 6:724–730. [PubMed: 12808460]

Smith MD, Yang XH, Nha JY, Buccafusco JJ. Antinociceptive effect of spinal cholinergic stimulation: interaction with substance P. Life Sci. 1989; 45:1255–1261. [PubMed: 2478855]

Talley EM, Cribbs LL, Lee JH, Daud A, Perez-Reyes E, Bayliss DA. Differential distribution of three members of a gene family encoding low voltage-activated (T-type) calcium channels. J Neurosci. 1999; 19:1895–1911. [PubMed: 10066243]

Tata AM, Vilaro MT, Mengod G. Muscarinic receptor subtypes expression in rat and chick dorsal root ganglia. Brain Res Mol Brain Res. 2000; 82:1–10. [PubMed: 11042353]

Veves A, Backonja M, Malik RA. Painful diabetic neuropathy: epidemiology, natural history, early diagnosis, and treatment options. Pain Med. 2008; 9:660–674. [PubMed: 18828198]

Wang XL, Zhang HM, Chen SR, Pan HL. Altered synaptic input and GABAB receptor function in spinal superficial dorsal horn neurons in rats with diabetic neuropathy. J Physiol. 2007; 579:849–861. [PubMed: 17218355]

Wanke E, Bianchi L, Mantegazza M, Guatteo E, Mancinelli E, Ferroni A. Muscarinic regulation of Ca2+ currents in rat sensory neurons: channel and receptor types, dose-response relationships and cross-talk pathways. Eur J Neurosci. 1994; 6:381–391. [PubMed: 8019675]

Wess J. Molecular biology of muscarinic acetylcholine receptors. Crit Rev Neurobiol. 1996; 10:69–99. [PubMed: 8853955]

Wu ZZ, Cai YQ, Pan HL. A functional link between T-type calcium channels and mu-opioid receptor expression in adult primary sensory neurons. J Neurochem. 2009; 109:867–878. [PubMed: 19250340]

Zhang HM, Chen SR, Pan HL. Regulation of glutamate release from primary afferents and interneurons in the spinal cord by muscarinic receptor subtypes. J Neurophysiol. 2007a; 97:102–109. [PubMed: 17050831]

Zhang HM, Li DP, Chen SR, Pan HL. M2, M3, and M4 receptor subtypes contribute to muscarinic potentiation of GABAergic inputs to spinal dorsal horn neurons. J Pharmacol Exp Ther. 2005; 313:697–704. [PubMed: 15640398]

Zhang HM, Zhou HY, Chen SR, Gautam D, Wess J, Pan HL. Control of glycinergic input to spinal dorsal horn neurons by distinct muscarinic receptor subtypes revealed using knockout mice. J Pharmacol Exp Ther. 2007b; 323:963–971. [PubMed: 17878406]

Zhuo M, Gebhart GF. Tonic cholinergic inhibition of spinal mechanical transmission. Pain. 1991; 46:211–222. [PubMed: 1661000]

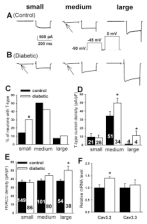

Figure 1.

Changes in the activity of T-type VACCs and HVACCs in DRG neurons of diabetic rats. **A, B**: typical traces show T-type (indicated by arrows) and HVACC I_{Ba} in small, medium, and large DRG neurons from control and diabetic rats. **C**: summary data show the percentage of small, medium, and large DRG neurons with T-type I_{Ba} in control and diabetic rats. **D**: group data show the current density of T-type I_{Ba} of control and diabetic rats. **E**: summary data show the current density of HVACCs of DRG neurons in control and diabetic rats. **F**: group data show changes in the mRNA level of Cav3.2 and Cav3.3 subtypes in the DRG from control and diabetic rats (n= 6 samples in each group). Data were presented as mean ± SEM. **P* < 0.05, compared with the control group.

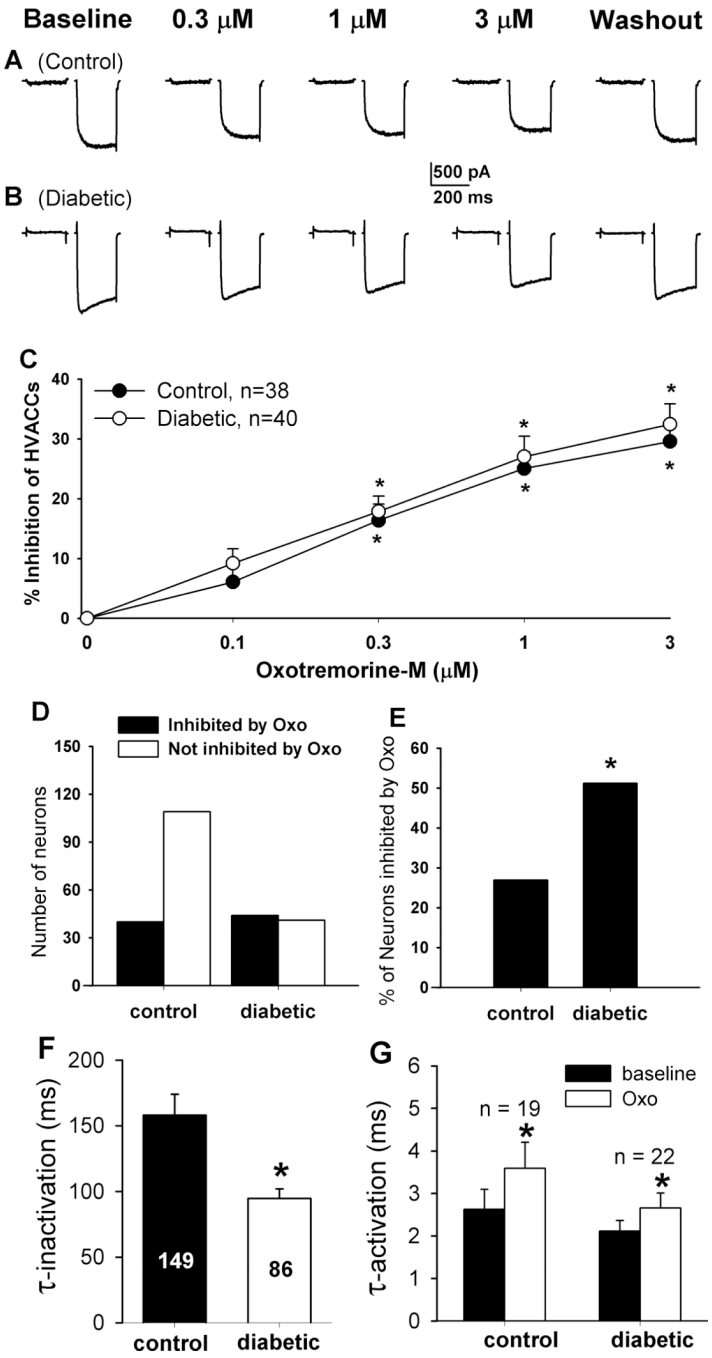

Figure 2.

Effects of Oxo-M on HVACC I_{Ba} in small DRG neurons from control and diabetic rats. **A, B**: original traces show that Oxo-M dose-dependently inhibited HVACC I_{Ba} in small DRG neurons from control and diabetic rats. **C**: summary data show the dose-response effect of Oxo-M on HVACC I_{Ba} in small DRG neurons from control and diabetic group. *$P < 0.05$, compared with the baseline before Oxo-M application. **D**: group data show the number of Oxo-M-responsive and Oxo-M-unresponsive small DRG neurons in control and diabetic rats. **E**: comparison of the percentage of Oxo-M-responsive small DRG neurons in control and diabetic rats. **F**: the inactivation time constant of HVACC currents in small DRG neurons in diabetic and control rats. **G**: effects of 1 μM Oxo-M on the activation time

constant of HVACCs in small DRG neurons in control and diabetic rats. *$P < 0.05$, compared with the control or baseline group.

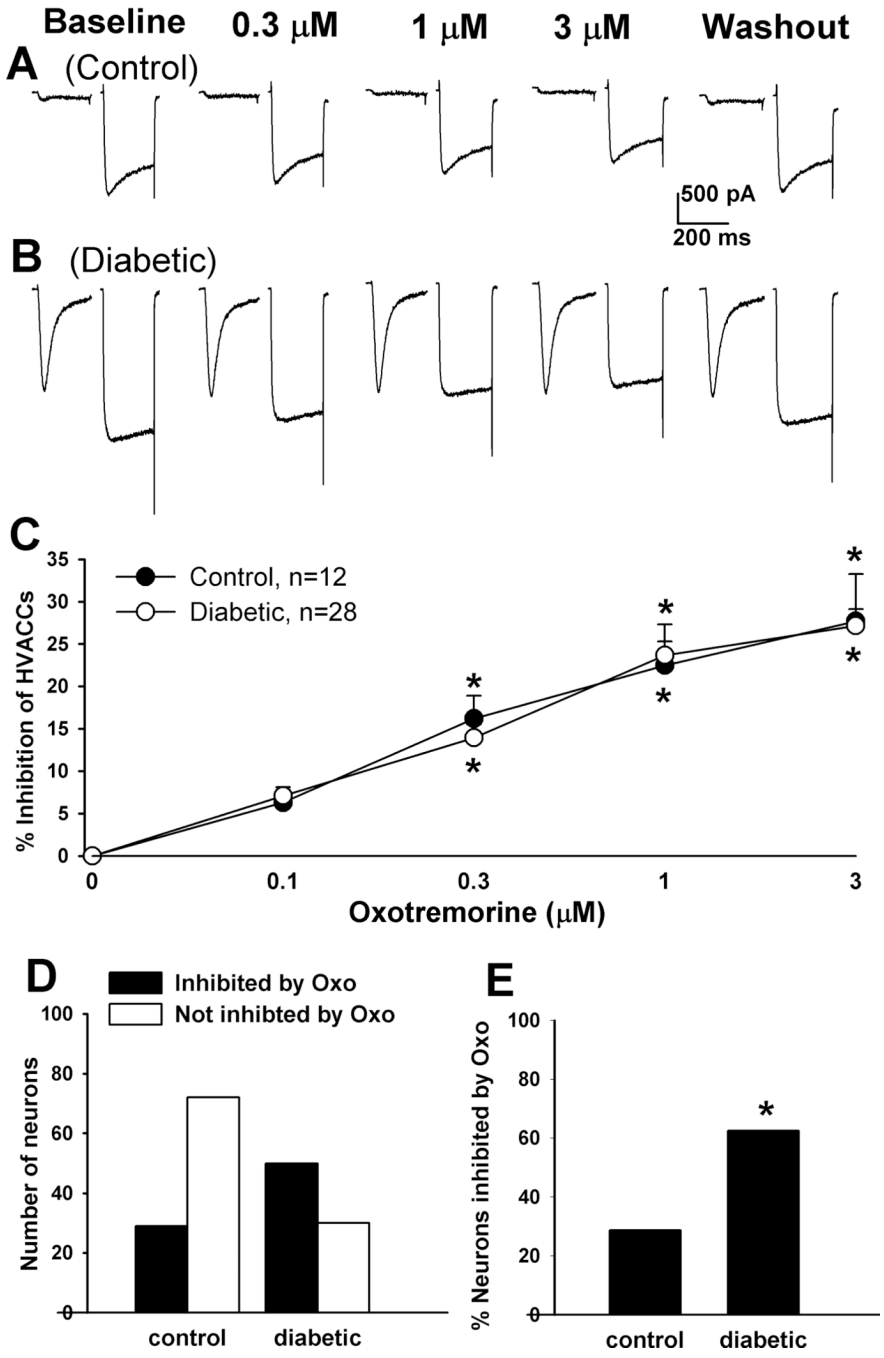

Figure 3.

Effects of Oxo-M on HVACC I_{Ba} in medium DRG neurons from control and diabetic rats. **A, B**: representative traces show that Oxo-M dose-dependently inhibited HVACC I_{Ba} in medium DRG neurons from control and diabetic rats. **C**: summary data show the dose-response effect of Oxo-M on HVACC I_{Ba} in medium DRG neurons from control and diabetic group. *$P < 0.05$, compared with the baseline before Oxo-M application. **D**: group data show the number of Oxo-M-responsive and Oxo-M-unresponsive medium DRG neurons in control and diabetic rats. **E**: comparison of the percentage of Oxo-M-responsive medium DRG neurons in control and diabetic rats. *$P < 0.05$, compared with the control group.

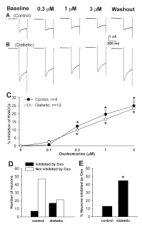

Figure 4.

Effects of Oxo-M on HVACC I_{Ba} in large DRG neurons from control and diabetic rats. **A, B**: original traces show that Oxo-M dose-dependently inhibited HVACC I_{Ba} in large DRG neurons from control and diabetic rats. **C**: summary data show the dose-response effect of Oxo-M on HVACC I_{Ba} in large DRG neurons from control and diabetic group. **P* < 0.05, compared with the baseline before Oxo-M application. **D**: group data show the number of Oxo-M-responsive and Oxo-M-unresponsive large DRG neurons in control and diabetic rats. **E**: comparison of the percentage of Oxo-M-responsive large DRG neurons in control and diabetic rats. **P* < 0.05, compared with the control group.

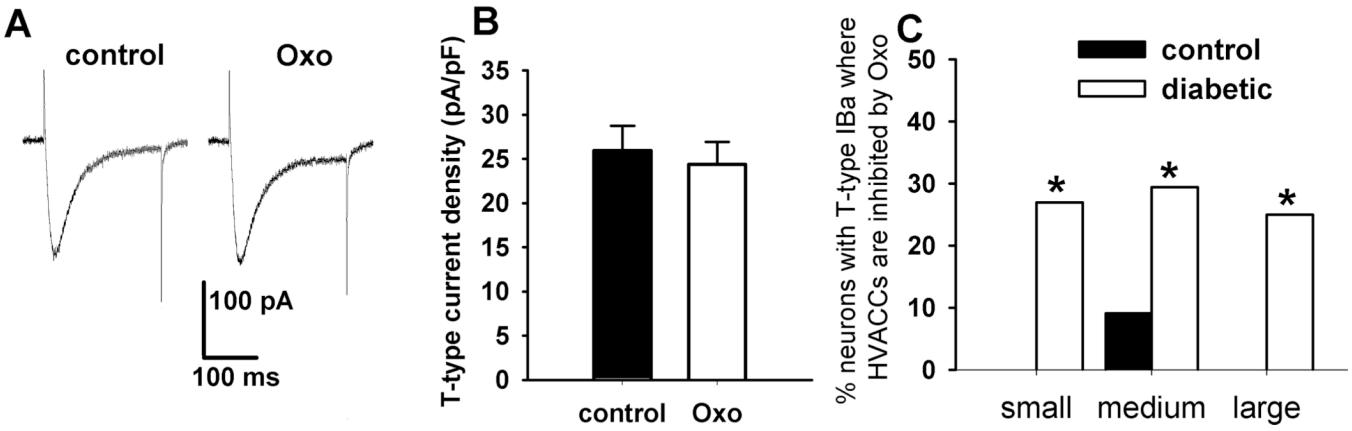

Figure 5.

Lack of effects of Oxo-M on T-type I_{Ba} in DRG neurons from control and diabetic rats. **A**: original traces show that 1 μM Oxo-M had no effect on T-type I_{Ba} in a medium DRG neuron from a diabetic rat. **B**: group data show that Oxo-M had no effect on the current density of T-type I_{Ba} in a total of 140 DRG neurons from control and diabetic rats. **C**: summary data show the percentage of neurons with T-type I_{Ba} inhibited by 1 μM Oxo-M in control and diabetic rats. *$P < 0.05$, compared with the control group.

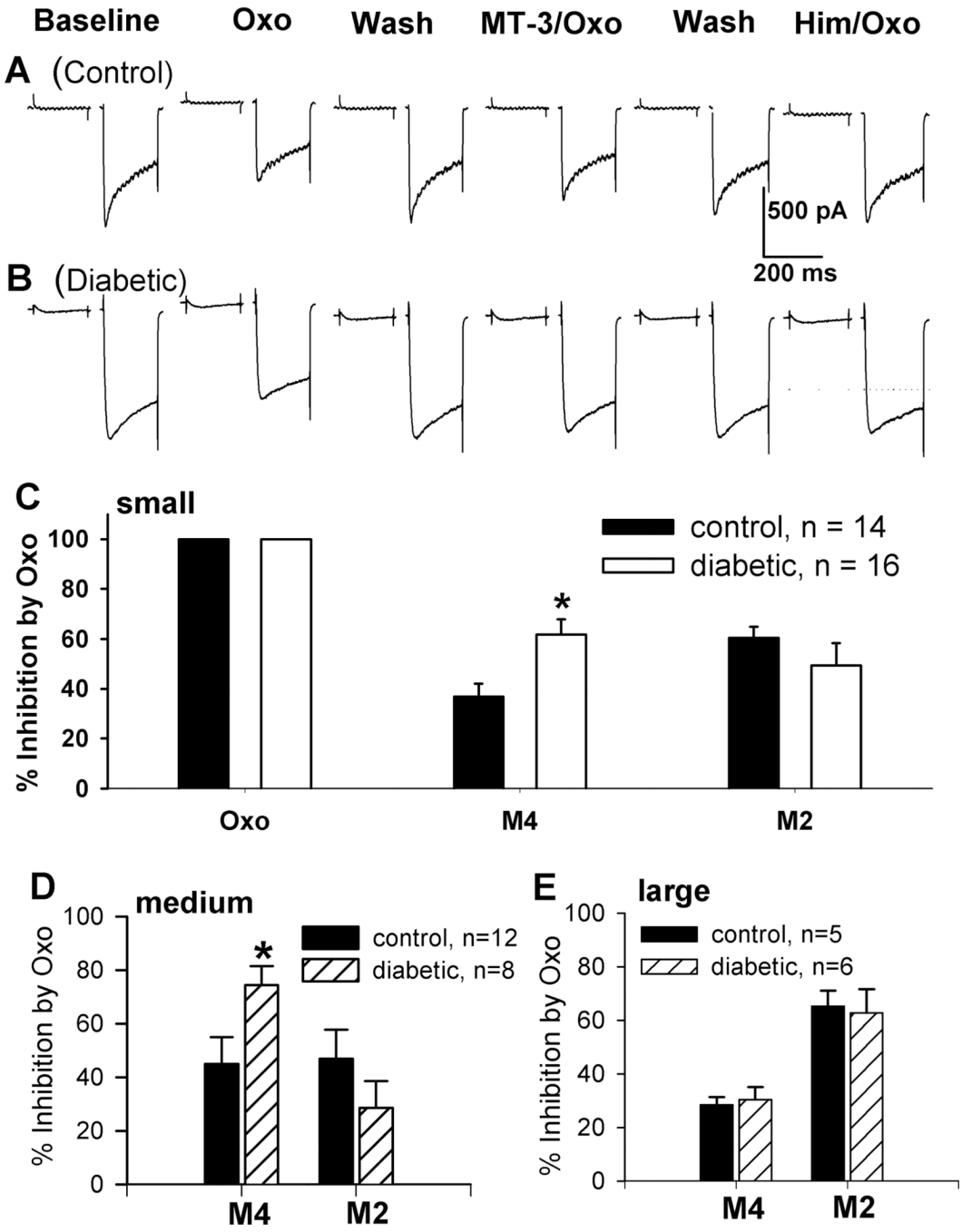

Figure 6.

Contribution of M_2 and M_4 subtypes to inhibition of HVACC I_{Ba} by Oxo-M in DRG neurons from control and diabetic rats. **A, B**: representative traces show the effect of 1 μM Oxo-M on HVACC I_{Ba} in the presence of 50 nM MT-3 or 2 μM himbacine in small DRG neurons from a control and a diabetic rat. **C**: comparison of the contribution of M_2 and M_4 subtypes to inhibition on HVACC I_{Ba} by Oxo-M in small DRG neurons from control and diabetic rats. **D**: summary data show M_2- and M_4-mediated inhibition of HVACC I_{Ba} by Oxo-M in medium DRG neurons from control and diabetic rats. **E**: group data show M_2- and M_4-mediated inhibition of HVACC I_{Ba} by Oxo-M in large DRG neurons from control and diabetic rats. *$P < 0.05$, compared with the control group.

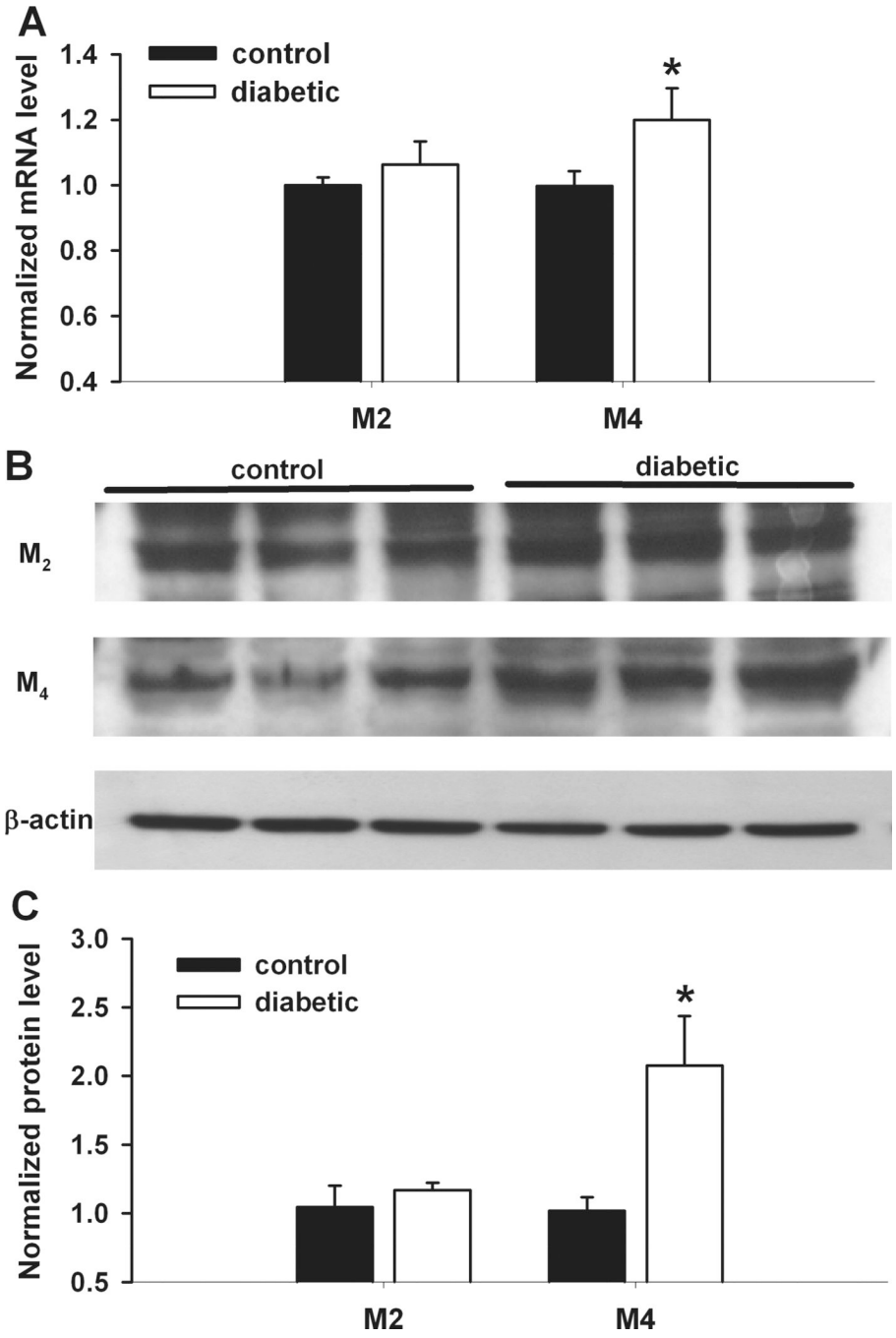

Figure 7.

Changes in the mRNA and protein levels of M_2 and M_4 subtypes in the DRG of diabetic rats. **A:** group data show the difference in the mRNA level of M_2 and M_4 subtypes in the DRG between control and diabetic rats (n = 6 samples in each group). **B**: original gel images show the protein level of M_2 and M_4 subunits in the DRG from control and diabetic rats. **C**: summary data show the M_2 and M_4 protein levels in the DRG from control and diabetic rats (n = 6 samples in each group). *$P < 0.05$, compared with the control group.

Table 1

List of primers used for real-time PCR analysis.

Gene	Primer	Sequence	Location
Rat-M_2	M_2-R1	5' tcccgggcaagcaagagtagaataaaga 3'	1079–1106
(NM_031016)	M_2-R2	5' ccaggccgccatcaccaccag 3'	1217–1197
Rat-M_4	M_4-R1	5' gcccctgggtgccgtggtctgtga 3'	765–788
(XM_001078223)	M_4-R2	5' ggcgggcgggataggtgaggggtttg 3'	901–87
Rat-Cav3.2	Cav3.2-P1	5' cgccggccctactacgcagactattc 3'	4831–4856
(NM_153814)	Cav3.2-P2	5' atgatgcggatgatggtgggattgat 3'	5195–5170
Rat-Cav3.3	Cav3.3-P1	5' tgggcgagatgacactgaagg 3'	3524–3544
(NM_020084)	Cav3.3-P2	5' aggatgccgaagatgatgaagaag 3'	3845–3822